

Charge Transfer Relaxation in Donor-Acceptor Type Conjugated Materials

By *Mariateresa Scarongella, Andrey Laktionov, Ursula Rothlisberger and Natalie Banerji**

Supporting Information

[*] M. Scarongella, Dr. N. Banerji
Photochemical Dynamics Group
Institute of Chemical Sciences & Engineering
Ecole Polytechnique Fédérale de Lausanne
CH-1015 Lausanne (Switzerland)
E-mail: natale.banerji@epfl.ch.

A. Laktionov, Prof. U. Rothlisberger
Laboratory of Computational Chemistry and Biochemistry
Institute of Chemical Sciences & Engineering
Ecole Polytechnique Fédérale de Lausanne
CH-1015 Lausanne (Switzerland)

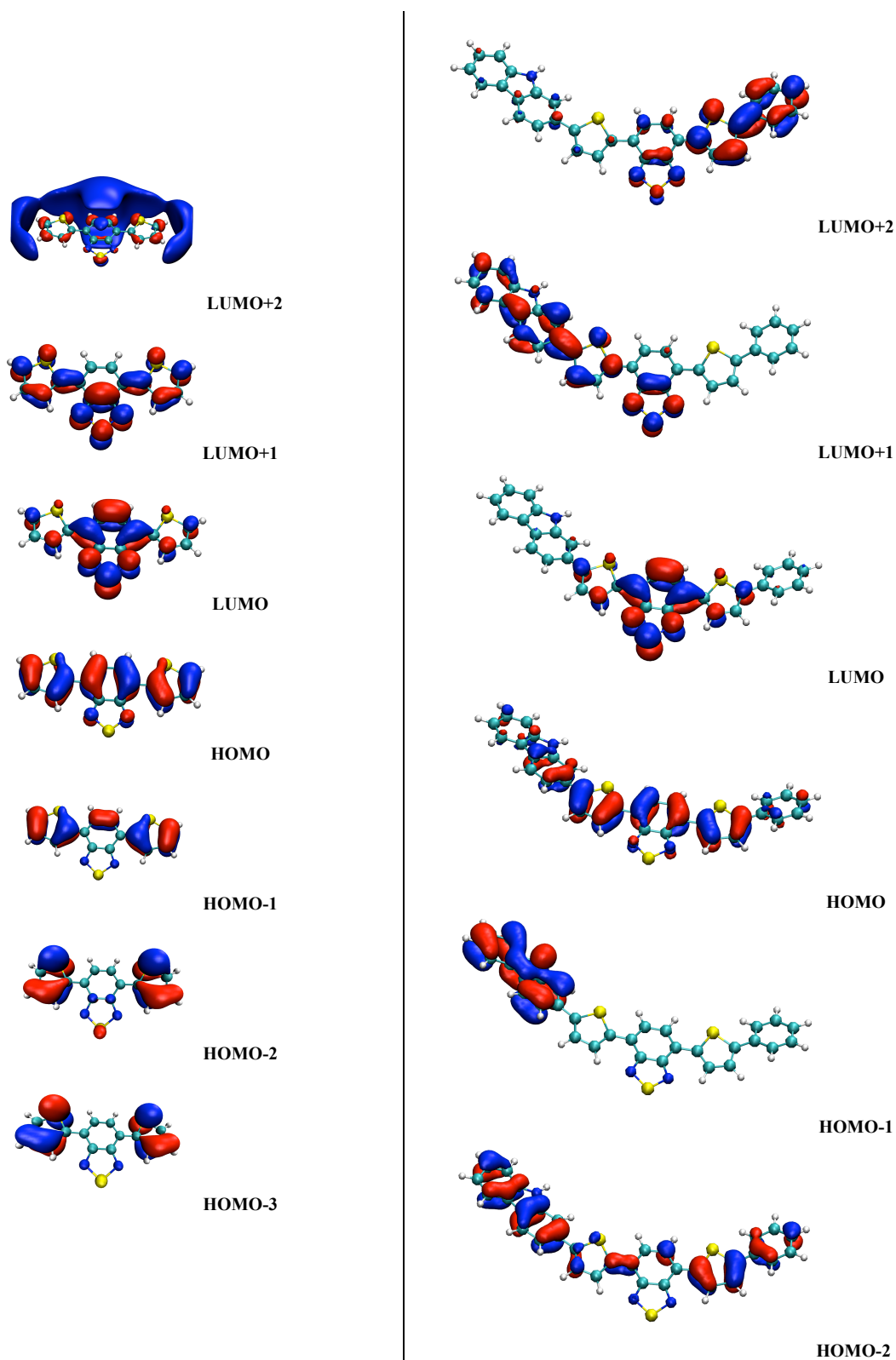
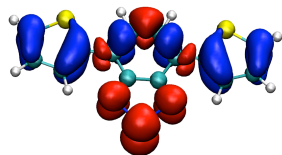
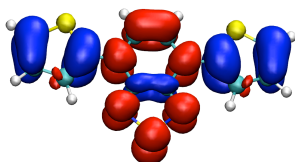


Figure S1. Molecular orbitals of dTBT (left) and CDTBT (right) calculated by TD-DFT (M062X/6-31+G*, gas phase). Geometries were previously optimized using B3LYP/6-31G**.

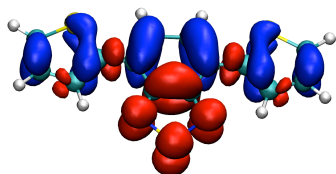
$S_0 \rightarrow S_1$ 2.8146 eV $f=0.4434$
 HOMO \rightarrow LUMO 0.70160



$S_0 \rightarrow S_2$ 4.2164 eV $f=0.0351$
 HOMO-4 \rightarrow LUMO 0.17433
 HOMO-2 \rightarrow LUMO -0.14419
 HOMO-1 \rightarrow LUMO 0.65451

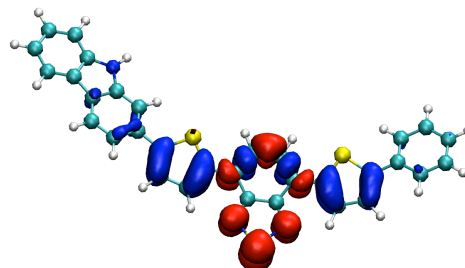


$S_0 \rightarrow S_3$ 4.3570 eV $f=0.3822$
 HOMO-3 \rightarrow LUMO -0.24556
 HOMO-1 \rightarrow LUMO+2 -0.11164
 HOMO \rightarrow LUMO+1 0.64055

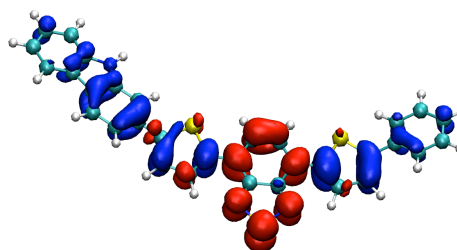


$S_0 \rightarrow S_4$ 4.3596 eV $f=0.0372$
 $S_0 \rightarrow S_5$ 4.5390 eV $f=0.1053$
 $S_0 \rightarrow S_6$ 4.5804 eV $f=0.0980$

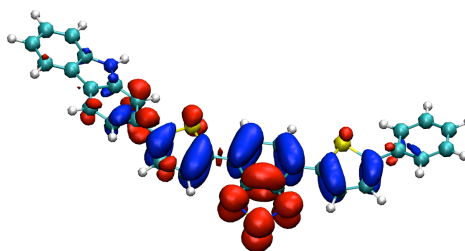
$S_0 \rightarrow S_1$ 2.5159 eV $f=1.0178$
 HOMO \rightarrow LUMO 0.68801



$S_0 \rightarrow S_2$ 3.5502 eV $f=0.1873$
 HOMO-8 \rightarrow LUMO -0.10020
 HOMO-3 \rightarrow LUMO 0.15910
 HOMO-2 \rightarrow LUMO 0.63603
 HOMO \rightarrow LUMO+1 -0.16182

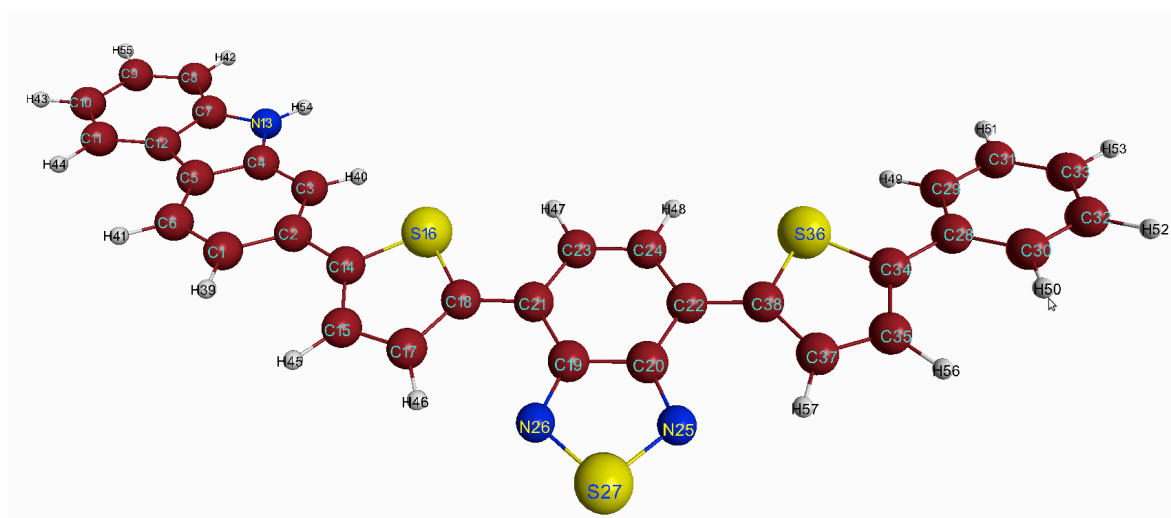


$S_0 \rightarrow S_3$ 3.7816 eV $f=0.8788$
 HOMO-3 \rightarrow LUMO 0.13393
 HOMO-2 \rightarrow LUMO 0.11809
 HOMO-2 \rightarrow LUMO+2 -0.16665
 HOMO \rightarrow LUMO+1 0.60140
 HOMO \rightarrow LUMO+2 -0.19309



$S_0 \rightarrow S_4$ 3.8684 eV $f=0.0086$
 $S_0 \rightarrow S_5$ 4.0762 eV $f=0.2077$

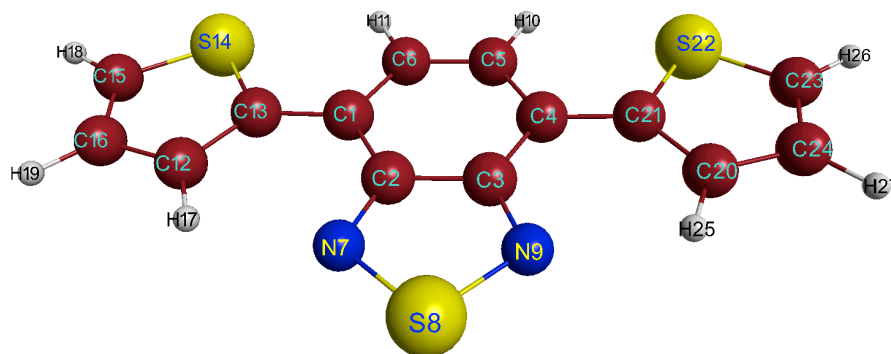
Figure S2. TD-DFT absorption transitions obtained for dTBT (left) and CDTBT (right) in the gas phase at the M062X/6-31+G* level of theory. Excitation energies, oscillator strengths and decomposition into single-particle transitions with corresponding weight are given for each excited state. For the first three transitions, the difference between the excited and ground state electron density calculated for vertical absorption are also shown.



Degree of freedom	Ground state geometry	Excited state geometry
C21-C22	2.946	2.913
C18-C38	5.866	5.760
C22-C24	1.377	1.423
C23-C24	1.421	1.375
C21-C23	1.377	1.424
C19-C21	1.441	1.439
C20-C19	1.451	1.449
C20-C22	1.441	1.438
C20-C22-C24	115.126°	116.741°
C35-C34-C28-C30	-29.056°	-20.291°
C15-C14-C2-C1	29.586°	16.664°
C19-C21-C18-C17	-15.161°	-0.536°
C20-C22-C38-C37	14.849°	0.773°
C6-C5-C12-C11	0.023°	0.038°

Root mean square deviation (RMSD) = 0.22 Å (calculated for fitted geometries)

Figure S3. Numbering scheme and representative bond lengths (in Angstrom) and angles (in degrees) for the ground state geometry and relaxed S_1 excited state geometry of CDTBT in the gas phase.



Degree of freedom	Ground state geometry	Emitting state geometry
C1-C4	2.951	2.900
C4-C5	1.376	1.428
C3-C4	1.441	1.436
C5-C6	1.421	1.373
C3-N9	1.331	1.332
C4-C21	1.463	1.427
C20-C21	1.376	1.397
N9-S8	1.621	1.663
C3-C4-C5	114.890°	114.226°
C2-C1-C13-C12	0°	0°
C3-C4-C21-C20	0°	0°

Root mean square deviation (RMSD) = 0.05 Å (calculated for fitted geometries)

Figure S4. Numbering scheme and representative bond lengths (in Angstrom) and angles (in degrees) for the ground state geometry and relaxed S₁ excited state geometry of dTBT in the gas phase.

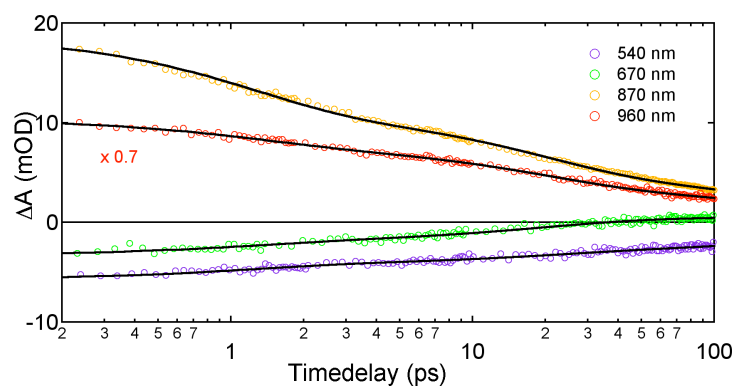


Figure S5. Transient absorption dynamics of CDTBT thin film at selected probe wavelengths, following excitation at 510 nm (solid lines represent the best multiexponential global fit).

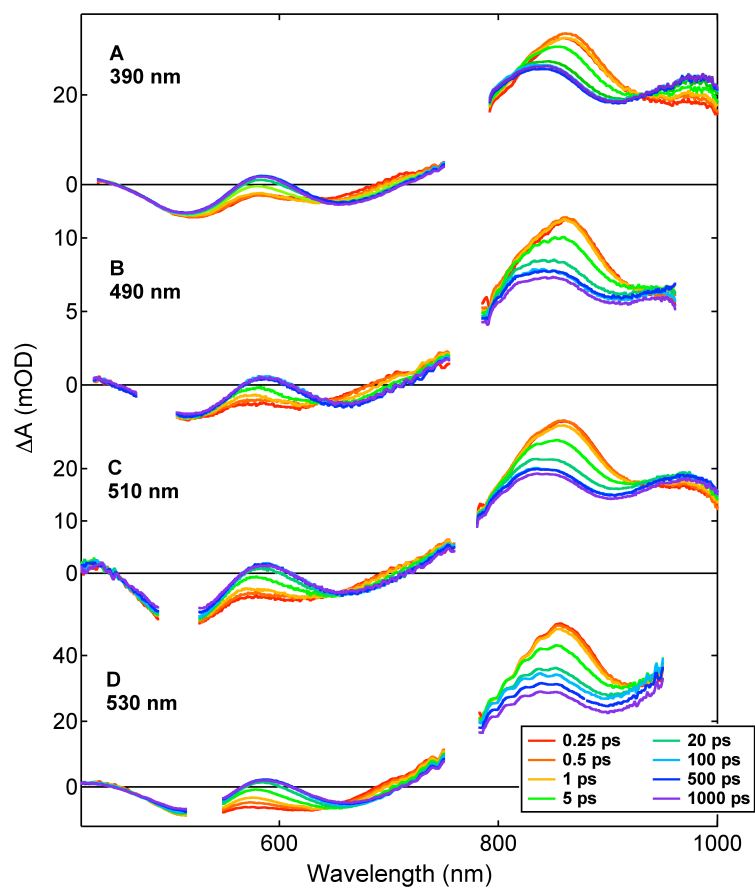


Figure S6. Transient absorption spectra of CDTBT in DCB at various time delays following excitation at 400 nm, 490 nm, 510 nm and 530 nm.

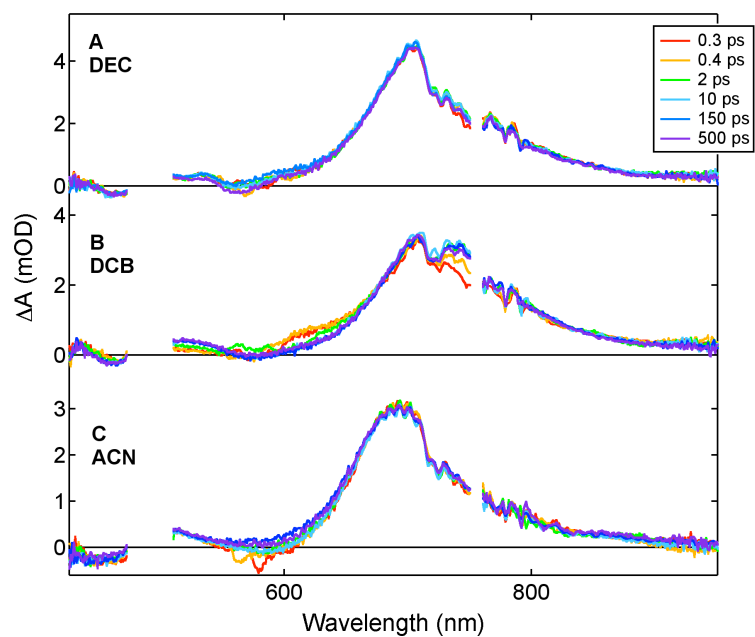


Figure S7. Transient absorption spectra of dTBT in different solvents, recorded at various time delays following excitation at 490 nm.

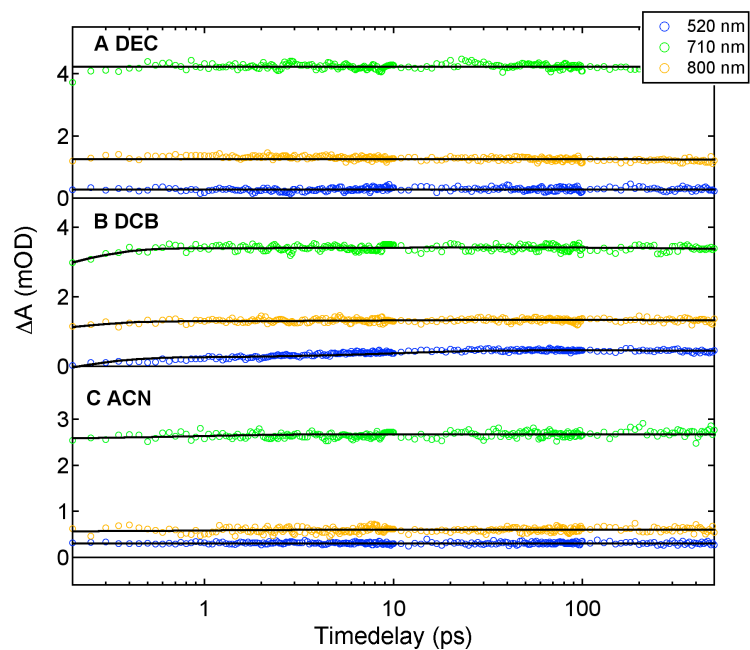


Figure S8. Transient absorption dynamics of dTBT in different solvents at selected probe wavelengths, following excitation at 490 nm (solid lines represent the best multiexponential global fit).

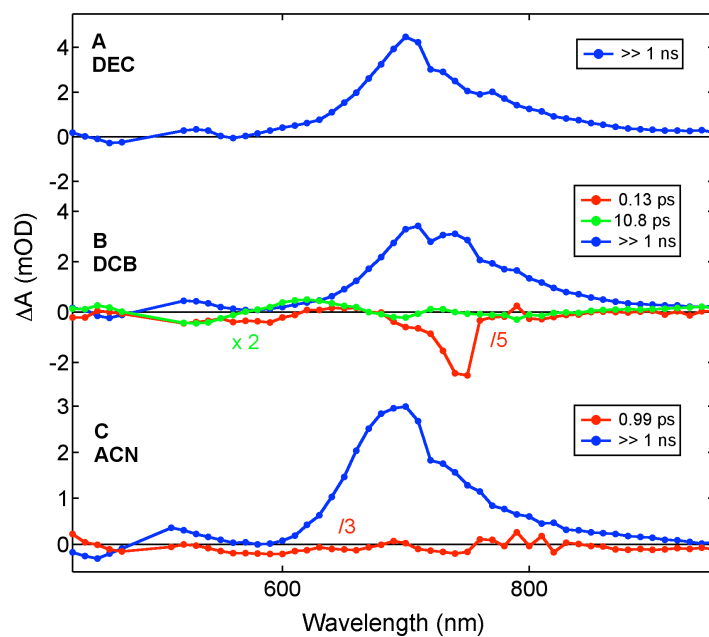


Figure S9. Amplitude spectra associated with the time constants resulting from a multiexponential global analysis of the transient absorption dynamics of dTBT in different solvents, recorded following excitation at 490 nm.